Steady and transient natural convection experiments in a horizontal porous layer: The effects of a thin top fluid layer and oscillating bottom wall temperature

Michael Kazmierczak and Arun Muley
Department of Mechanical, Industrial, and Nuclear Engineering, University of Cincinnati, Cincinnati, OH, USA

Natural convection in a horizontal porous layer heated from below was experimentally investigated. Two types of experiments were carried out. First, steady-state experiments in the range $200 < Ra < 1{,}000$ are reported, and the results are discussed in the framework of previously published works. Two types of upper surface conditions are explored, "the clear top layer case" and the completely packed enclosure, and the effect on the heat transfer through the enclosure is examined. Next, a series of unique transient experiments were conducted and are reported in which the bottom wall temperature cyclically changes. The period varies from approximately 6 to 180 min, and the amplitude of the bottom wall temperature oscillation ranges from 3 to 45 percent of the enclosure's mean temperature difference. The temperature of the upper surface was maintained constant in all of these transient runs, and both cases of upper boundary conditions are studied. The results of the steady-state experiments showed that the type of top boundary condition significantly affects the Nusselt number *versus* Rayleigh number relationship. It was found that the steady-state heat-transfer rate through the enclosure is greater in the porous layer containing a thin top fluid layer. The transient experiments showed that the cycle-averaged heat-transfer rate through the layer is different from its steady-state value when the bottom wall temperature oscillates. The heat transfer may increase or decrease, which depends strongly on the kind of upper surface condition. The effects of the period and the amplitude of the wall temperature modulation are examined and are documented for both surface conditions.

Keywords: porous media; steady and transient free convection; horizontal enclosure

Introduction

Convection in porous media has been extensively studied in the past, motivated by a wide range of applications such as storage and recovery of energy, geothermal engineering, heat exchangers and heat-transfer augmentation, insulation of buildings, solidification of alloys, nuclear waste disposal, and storage of heat-generating materials such as grains and coals. A review of the early works on the subject, which also includes a detailed account of natural convection in a horizontal porous layer heated from below (the subject of the present focus), can be found in Combarnous and Bories (1975) and Cheng (1978). Nield and Bejan (1992) updated these early review articles, incorporating the very latest research and theories in porous media in a recently published book.

The aim of this article is to report an experimental investigation of the heat transfer in a rectangular enclosure filled with a saturated porous medium heated from below with and without a thin top fluid layer. This study consists of two parts: the steady-state heat transfer through the enclosure with constant bottom wall temperature and the transient natural convection phenomenon when the bottom wall temperature changes cyclically with time.

A large body of literature exists that examines convection in the porous system with steady boundary conditions. Although numerous experimental studies (Buretta and Berman 1976; Elder 1967; Lister 1990) have been conducted, conflicting results have fueled a controversy in porous media convection that is more than 20 years old, which remains unresolved today. Over the years, many numerical studies (Caltagirone 1975; Elder 1967; Kladias and Prasad 1989b) have added insight to this debate, but they alone cannot clarify the issues because the equations governing momentum and energy transport in a porous medium themselves are not without question (Lage 1992). In addition, complicating the problem is the fact that the convection phenomenon occurring in the porous layer may not necessarily be steady, even though the boundary conditions are constant. Stable convection, oscillatory periodic, and oscillatory chaotic are all different types of flow regimes that are known to occur (Caltagirone 1975; Caltagirone and Fabrie 1989; Kladias and Prasad 1990; Schubert and Straus 1979). For a more complete discussion of the latest research on this particular problem, see Nield and Bejan (1992).

Address reprint requests to Professor Kazmierczak at the Department of Mechanical, Industrial, and Nuclear Engineering, University of Cincinnati, Cincinnati, OH 45221-0072, USA.

Received 18 February 1993; accepted 9 July 1993

In contrast to the preceding, convection in a horizontal porous layer with time-dependent bottom heating has received very little attention. This fact is rather surprising because unsteady boundary conditions are more often the rule than the exception when dealing with natural occurring processes. The *step change* in bottom wall temperature has been investigated by Elder (1968), Holst and Aziz (1972), and others, but their focus was on the evolution to and on the final steady-state behavior. The only published transient studies that we are aware of with a *continually changing* bottom wall temperature involve stability-type problems. Kaviany (1984) experimentally and theoretically studied the onset time for convection in a horizontal layer whose lower surface temperature increased linearly with time. The case in which the temperature imposed on the lower boundary is timewise periodic was analyzed by Chhuon and Caltagirone (1979). Using linear stability theory, they developed a criterion for the onset of convection defined in terms of the perturbation wave number, amplitude, and frequency of the temperature oscillation.

The steady-state experiments (first part of this study) add to the existing database, but of greater significance they document the importance of good packing and filling of spherical beads (porous medium) in the enclosure, and show what happens when a small gap remains. The transient experiments (second half of this study) explore the effect of bottom wall temperature modulation at above-critical Rayleigh numbers and represent a first study of this kind in convective porous medium research.

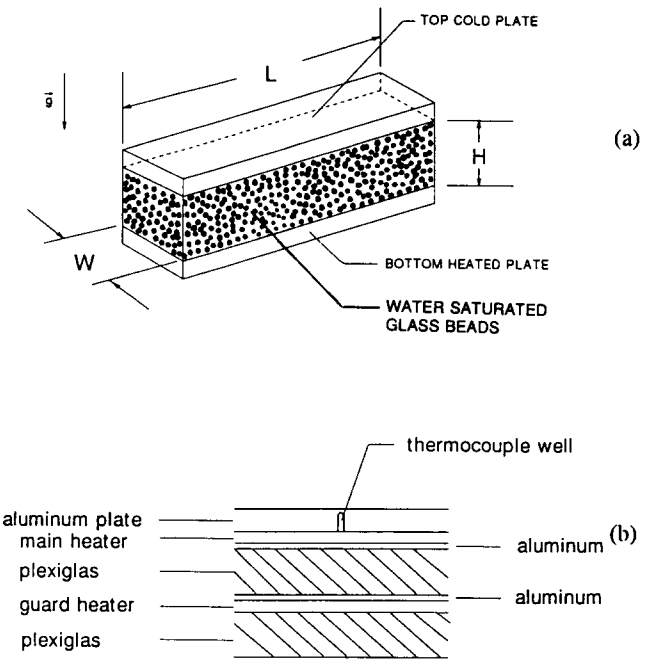

Figure 1 Experimental apparatus: (a) isometric sketch; and (b) cross section of heated bottom plate

Experimental apparatus

Test cell

The experiments were performed in the rectangular enclosure shown schematically in Figure 1a. This apparatus is the same as that used by Mantle-Miller et al. (1992) in an earlier study of transient natural convection of a pure fluid. The height to length aspect ratio was 1:4, with its internal dimensions measuring 50.8 cm long × 12.7 cm deep × 12.7 cm high. The vertical side walls were constructed out of 1.91-cm-thick clear Plexiglas, and the top and bottom horizontal driving surfaces were machined from thick aluminum plates.

The top wall of the enclosure was cooled by circulating cold tap water through five large channels that were milled lengthwise along the top plate. To ensure isothermality of the top plate, the water was made to travel in opposite directions in adjacent channels and was circulated at a very high flow rate. The temperature of the upper wall was measured using eight 30-gauge type T thermocouples that were embedded to a depth of 0.16 cm from the inside surface.

The bottom plate was constructed in a "sandwich" fashion. The cross section showing the different layers making up the bottom hot plate is drawn in Figure 1b. The upper layer was made from 1.3-cm-thick aluminum plate and was heated by a 13.6 Ω resistance flexible rubber main heater located directly underneath. To prevent heat transfer from going downward and out from the bottom of the enclosure, a second or "guard" heater was used. The main heater and the guard heater were separated by a 2.54-cm-thick insulating Plexiglas layer. Sandwiched between the heaters and the Plexiglas layer were thin (0.3-mm-thick) aluminum plates to help smooth out the temperature irregularities of the heaters. In addition, highly conductive paste was placed between all layers to enhance the thermal contact. Finally, 2.54-cm-thick Plexiglas was added below the guard heater for insulation. Thermocouples were

Notation

A	Area of heated surface, m^2
Amp	Amplitude of temperature change, °C
Da	Darcy number, Equation 3
d	Diameter of glass bead, m
g	Gravitational acceleration, m/s^2
H	Enclosure height, m
k	Overall thermal conductivity of porous medium, Equation 5, W/m °C
K	Permeability of porous medium, Equation 2, m^2
L	Enclosure length, m
Nu	Nusselt number, Equation 4
Pr	Prandtl number, ν/α
Q	Heat-transfer rate, W
Ra	Rayleigh number, Equation 1
T	Temperature, °C

Greek symbols

α	Thermal diffusivity, m^2/s
β	Coefficient of volumetric thermal expansion, K^{-1}
ε	Porosity of porous medium
ν	Kinematic viscosity, m^2/s
ρ	Fluid density, kg/m^3

Subscripts

c	Cold (top) wall
f	Fluid
h	Hot (bottom) wall
p	Porous
s	Solid

Superscript

Denotes the quantity is averaged over time

embedded in the upper aluminum plate (within 0.16 cm from inside surface) and in each of the thin aluminum plates located next to the heaters. The upper thermocouples were used to measure the bottom wall temperature, and the thermocouples in the thin aluminum plates were used to record the heater temperatures. The enclosure was mounted (and leveled) on a sturdy work table. To prevent heat loss, an insulation jacket made from 9.5-cm-thick styrofoam board surrounded the enclosure and insulated the top and all sides.

The enclosure was filled with a porous medium in all of the experiments. The porous matrix consisted of 3-mm spherical glass beads saturated with deionized water. Care was taken in filling the enclosure with the glass beads and water mixture and in securing the top plate. For the completely packed experiments it was essential that the glass beads were in direct contact with the top plate. This was done by filling the test section with beads and fluid to a level slightly above the side walls (approximately 1–2 bead diameters), and then by compressing the porous matrix by attaching the top plate. Despite this precaution, it was noted, however, that a small gap had developed at the top plate during the course of the preliminary runs, apparently because of settling of the beads. This resulted in a thin (approximately 3–5-mm) fluid layer devoid of beads adjacent to the inside surface of top plate. Nevertheless, steady-state and transient experiments were run with this top surface condition, which, hereafter, will be referred to as the clear top layer case. To study the completely packed top surface condition, more beads were added to the enclosure and then packed again as described previously. The second time, however, a gap never developed, and steady-state and transient runs were performed again in the porous layer.

For the enclosure filled with water saturated porous medium, the Rayleigh number is defined as (Bejan 1984)

$$\mathrm{Ra} = Kg\beta\Delta TH/\alpha v \tag{1}$$

where ΔT is the temperature difference between the cold (top) plate and hot (bottom) plates, K is the permeability of the porous medium, and all other variables are defined in the notation section. For randomly packed spherical beads it can be shown (Ergun 1952) that the permeability can be calculated by

$$K = d^2\varepsilon^3/180(1-\varepsilon)^2 \tag{2}$$

where

ε = porosity of porous medium

d = the bead diameter

The porosity was estimated to be $\varepsilon = 0.37$ and with $d = 3$ mm, Equation 2 gives $K = 6.38 \times 10^{-9}$ m^2. The Darcy number, or the dimensionless permeability, is defined as

$$\mathrm{Da} = K/H^2 \tag{3}$$

In our experiments, $\mathrm{Da} = 3.96 \times 10^{-7}$ and was fixed for all runs because only one combination of bead size and enclosure height was studied. For these conditions, the Rayleigh number of the enclosure varied from 100 to 1,100 for the steady-state and the transient runs.

Main heater electrical circuit

To oscillate the bottom wall temperature, the electric circuit shown in Figure 2a was used. This circuit was designed to periodically vary *power* to the main heater. The major components of the circuit included a variac, timer, an external (variable) resistor, and the primary main heater. The timer is basically a switch that opens and closes cyclically. The period

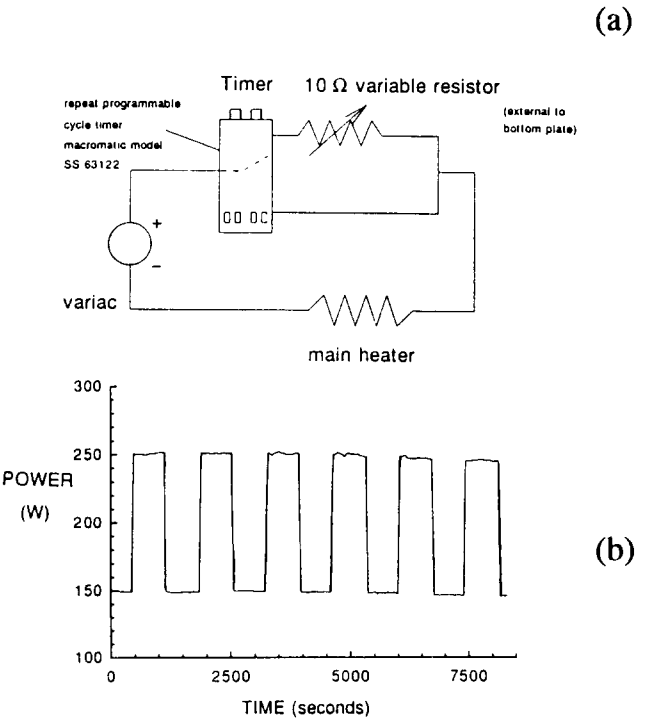

Figure 2 Electrical circuit used to modulate power to the main heater: (a) schematic writing diagram; and (b) measured power variation with time for typical experiments

is adjustable, using the top tuning knobs and by setting four dip switches located on the timer side, and can vary from 2.0 s to 24 h. When the timer switch is closed, the current passes through the variable resistor but is bypassed when the timer switch opens. Thus, the voltage drop across the main heater varies in a step fashion (Figure 2b) as the external resistor is switched in and out of the circuit by the timer. Thus, using the circuit just described, the *period* of the voltage oscillation is adjusted by changing the timer setting, whereas the *amplitude*, or the change in voltage drop across the main heater, is adjusted by changing the resistance of the external variable resistor.

The heat transfer through the cavity is reported in terms of the conduction-referenced Nusselt number. The Nusselt number is defined as

$$\mathrm{Nu} = Q_{\mathrm{average}}/(k\mathrm{A}\Delta T/H) \tag{4}$$

In this equation k is overall thermal conductivity of the porous matrix and was calculated as the weighted geometric mean of k_f and k_s, defined as (Nield 1992)

$$k = k_s^{1-\varepsilon}k_f^{\varepsilon} \tag{5}$$

Q_{average} in Equation 4 for the Nu number is the heat input and was calculated from the measured voltage drop across the primary heater and from the resistance of the primary heater. For the steady-state experiments Q_{average} was a constant value, but the power input varied in the transient experiments. There $Q_{\mathrm{average}} = Q_{\mathrm{cycle}}$ where Q_{cycle} was determined by numerically integrating the instantaneous Q over the period of the wall temperature oscillation.

Experimental procedure and data collection

The steady-state and transient experiments followed essentially the same basic procedure except for the steady-state experiments the timer and the external variable resistor in the

main electric circuit were removed. The main heater circuit was turned on, and the timer period and the resistance of external resistor was set. Cooling water was supplied to the cold plate, and the guard heater was turned on. As a rough estimate, the power to the guard heater was initially set at 5 percent of the main heater power. The system then ran for several cycles until the initial transient died and the time-averaged wall temperatures became nearly constant. A check was then made of the temperature of the guard heater. Because the guard heater was powered by a separate variac with constant output, the temperature of the guard heater was fixed, although the temperature of the main heater changed. The power to the guard heater was then adjusted until its temperature became equal to the minimum temperature experienced by the main heater. This reduced the heat loss through the bottom plate to the minimum level and prevented the power from the guard heater from contributing to the heat gain of the enclosure. Note that the guard to main heater temperature differential for the steady-state baseline experiments could be eliminated after making several fine adjustments to the guard heater. This was a time-consuming iterative process; so, instead, for many steady-state experiments, only one or two adjustments were made, just enough to get fairly close to the main heater temperature, and then power was corrected for the conduction heat loss through the bottom wall of the enclosure. The accuracy of this was checked by repeating several steady-state experiments, with and without bottom wall correction, and when compared gave practically identical results.

Once the final adjustments to the guard heater were made, the experimental data were logged. Each run took approximately one day to complete. In general, it was found that the system responded quickly, typically in just an hour or two, to changes made to the boundary condition, but care was exercised to ensure that the steady or the periodic solution was actually achieved. Typically, the transient experiments were run 10 to 40 cycles beyond the point where the main heater temperature, guard heater, and the mean bottom plate temperature became constant before reducing the data.

The data were automatically recorded using a HP 75000 data acquisition system driven by a 386/25-MHz personal computer running LabTech Notebook software. The raw data was sampled at 30-s intervals for most of the steady-state and transient runs. The data were then processed by a FORTRAN program, which calculated the mean temperature, amplitude, and the period of the driving walls. From the voltage drop data it calculated the cycled-averaged power to the main heater and, using the guard heater and main heater temperature data, corrected for heat loss resulting from conduction through the bottom plate. Finally, the Rayleigh number and the cycled-averaged Nu numbers of the experiments were calculated.

Results and discussion

Steady-state experiments: constant wall temperature

Twenty-five steady-state experiments were performed in which the hot plate temperature was held fixed. The runs with the enclosure completely packed with porous medium are reported in Table 1 and the runs in which a small gap was visible near the top plate (clear top-layer case) are reported in Table 2. The power to the main heater was maintained constant in all of the steady-state experiments and was incremented by 25 watts between runs. The Rayleigh number in the series of experiments ranged from approximately Ra = 200 to Ra = 1,000, and the corresponding steady-state Nusselt numbers, calculated via Equation 4, are listed in the fourth column of Table 1.

Table 1 Summary of steady-state experiments: completely packed case

Run	Power (W)	Ra	Nu
1	24.8	216.3	3.43
2	50.9	321.9	5.38
3	73.2	414.4	6.47
4	98.3	498.2	7.77
5	130.2	607.1	9.25
6	147.2	656.3	10.05
7	183.2	750.3	11.85
8	207.7	823.9	12.80
9	222.7	874.2	13.40
10	256.0	958.7	14.82
11	290.6	1051.9	16.04

Table 2 Summary of steady-state experiments: clear top-layer case

Run	Power (W)	Ra	Nu
1	26.97	187.88	5.87
2	51.63	294.90	7.96
3	72.99	379.71	9.34
4	103.32	481.93	11.11
5	132.60	569.27	12.99
6	144.14	609.11	13.45
7	173.17	673.40	15.23
8	200.63	750.98	16.47
9	225.47	785.36	17.97
10	254.05	868.34	18.95
11	268.57	887.09	19.71
12	301.17	966.30	21.19
13	324.12	998.74	22.37
14	351.84	1067.62	23.22

The results of these steady-state experiments are shown in Figures 3 and 4. Figure 3 shows Cheng's famous compilation of heat-transfer measurements (Cheng 1978) reported by nine earlier investigators with the present data superimposed. The "x" symbol denotes the current findings with the top figure corresponding to the case of no gap (i.e., enclosure completely filled with beads), and the data in the lower figure correspond to the experiments that contained a small ($\approx$3-mm) top gap. Inspection of Figure 3 shows that our data, for both cases considered, fit well within the spread of data published from the earlier researchers. More interesting, however, is the fact revealed by comparing our data set without gap (Figure 3a) to our data set with gap (Figure 3b). A better comparison of the two new data sets alone is shown in Figure 4, where only the present data are plotted on a single figure. Best-fit straight lines are drawn through both data sets to produce the correlations

$$\mathrm{Nu} = \mathrm{Ra}^{0.8145}/13.02 \tag{6}$$

$$\mathrm{Nu} = \mathrm{Ra}^{0.9554}/48.76 \tag{7}$$

Equation 6 applies to the clear top-layer case (triangular points), and Equation 7 applies to the completely packed data (square symbol). In addition to these two correlations the well-known equation

$$\mathrm{Nu} = \mathrm{Ra}/40 \tag{8}$$

is shown plotted as the dashed line in Figure 4. Clearly, the presence of a very small gap influences the heat transfer as shown by Figure 4. Two differences are readily apparent. First, the heat transfer through the enclosure is greater with the small

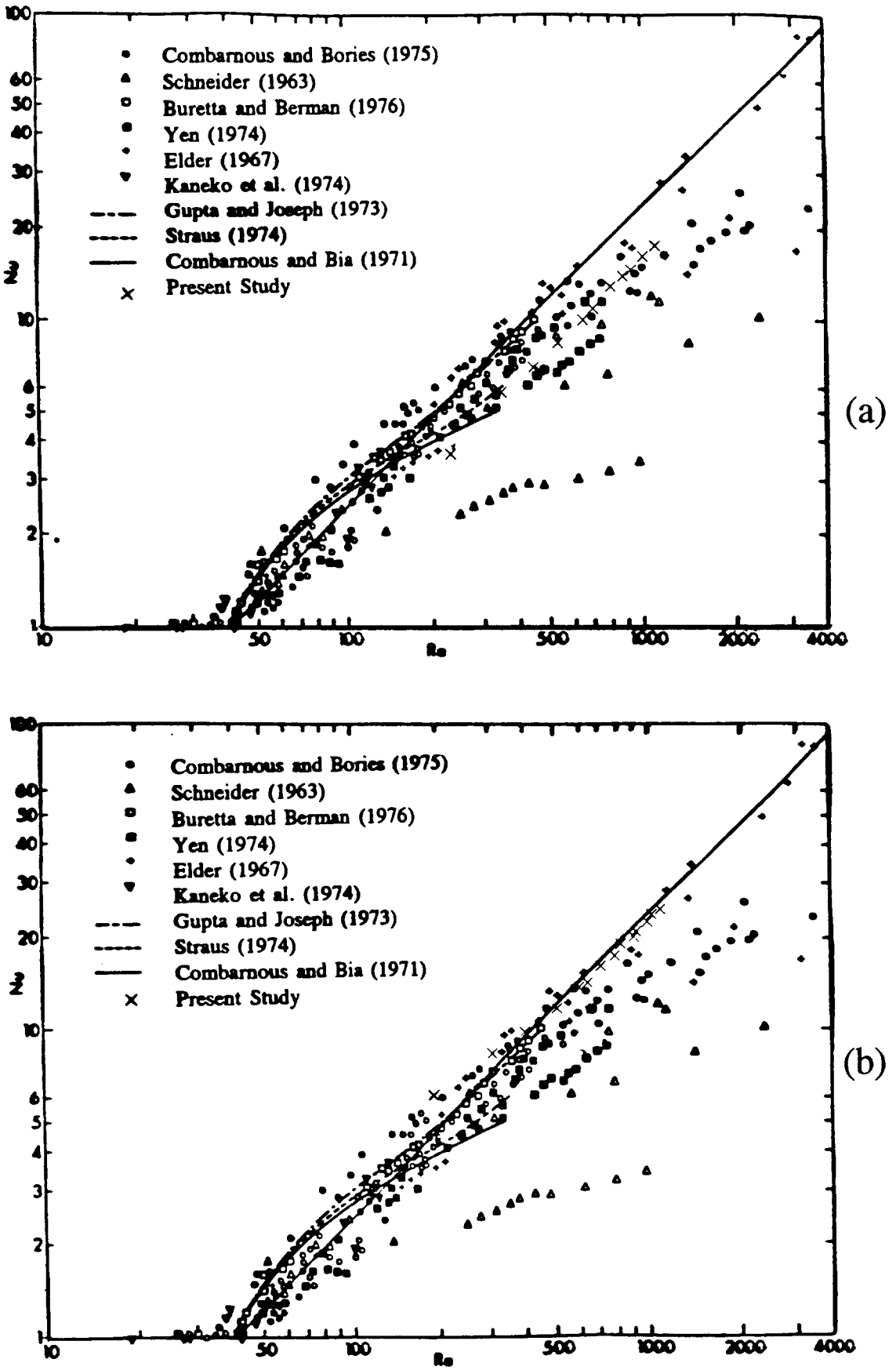

Figure 3 Summary of previous overall heat transfer measurements in fluid-saturated horizontal porous layer heated from below (Cheng 1978) with present data superimposed: (a) completely packed experiments (see Table 1); and (b) clear top-layer experiments (see Table 2)

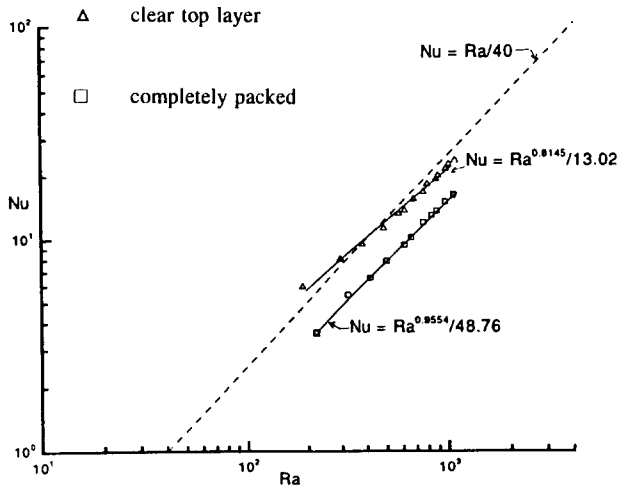

Figure 4 Nu *vs* Ra correlations for the steady-state experiments

gap than without it. Second, the gap causes the Rayleigh number dependence to change. The exponent in the Rayleigh number decreases from 0.9554 (completely packed experiments) to 0.8145 (clear top-layer case) just by adding a very small gap.

The first effect (i.e., the gap significantly increases the heat transfer) makes sense when the gap is viewed as reducing the flow resistance in the bed at the upper plate. This means more fluid flow occurs at the top plate, causing greater heat transfer. This behavior is akin to the well-established "channeling effect" in completely packed beds but is much more pronounced. In our case, the channeling is caused by the lack of beads rather than the exponential porosity variation in the beads caused by the presence of the wall. Poulikakos and Renken (1987) were the first two investigators to document the channeling effect in fully packed forced duct flows, and later Kladias and Prasad (1989a) showed that wall channeling also increases the heat transfer in buoyancy-driven cavity flows completely packed with a porous medium.

A significant difference in the slope of the Nu versus Ra curves for the different hydrodynamic boundary conditions is revealed in Figure 4. This is expected because different boundary conditions mean different flow fields and, therefore, perhaps, a different Rayleigh number dependence. For example, regarding the onset of convection, Nield (1968) showed that the boundary conditions greatly affect the stability of a horizontal porous layer heated from below, which, in turn, change the value of the critical Rayleigh number for convection. Ribando and Torrance (1976) and later Lein and Tankin (1992) also showed that the upper boundary condition affects the flow fields (and hence the heat-transfer rate) at above-critical Rayleigh numbers. Darcy flow for two different types of upper boundary confinement were numerically simulated in both of these studies, and both articles report marked differences in the flow pattern created by the change in the upper boundary condition. Ribando and Torrance studied a narrow cavity, $H/L = 1.67$, which contained only a single cell, but Lein and Tankin studied a shallow enclosure that contained multiple rolls. Their simulations showed that, for $30 < \mathrm{Ra} < 75$, the flow field with an impermeable top boundary condition (completely packed enclosure) contained eight cells, whereas only six cells were generated in the solution when a permeable upper surface condition was imposed. Finally, it is noted that both studies report an increase in the heat transfer of the permeable top case over the impermeable top condition primarily because of the strengthening of the flow field. To the best of our knowledge no published work has been done that showed the effect of the upper surface condition in the higher Ra number range considered in the present study.

The last issue to discuss in connection with Figure 4 is the dashed line. Elder (1967) was the first to propose the correlation given by Equation 8 to fit his experimental findings, and later Bejan (1984) showed that the linear variation can be predicted by simple scaling analysis assuming a Darcy flow model and a two-region cellular flow pattern. It must be clarified that Bejan's analysis and Elder's experiments were based on an enclosure completely filled with porous medium with no gap. Thus, it is appropriate to consider only the "square" symbols in Figure 4 in the discussion to follow. Comparing, we find our correlation, Equation 7, has nearly the same Rayleigh number dependence (0.96 *versus* 1), but the magnitude of heat transfer is less. The slope being constant and near 1 is significant and implies that the Darcy model is valid over the whole Rayleigh range investigated. This fact is not unexpected because the enclosure Darcy number for the experiment was very small. (Recall, $\mathrm{Da} = 3.96 \times 10^{-7}$). Note that this finding is also supported by the work of Kladias and Prasad (1989b) who numerically solved the Brinkman-Forchheimer extended Darcy equation of motion for a horizontal porous layer heated from below, and showed that for a densely packed medium with low permeability, $\mathrm{Da} < 10^{-4}$, the contribution from the inertia and viscous diffusion terms are negligible, and the Darcy flow model is acceptable. The difference in the magnitude of the heat transfer between our data and the dashed line is left unexplained. We emphasize that we were careful to eliminate the heat loss through the bottom plate by using a guard heater and that the rest of the enclosure was well insulated. Differences may be attributed to differences in the evaluation of the effective thermal conductivity of the porous matrix, which is known to have a fairly large value of uncertainty (Nield 1992). But, overall, keeping in mind the vast spread of data (Figure 3) encountered in this problem, we conclude that the difference is not at all unusual. In fact, note that our data for the completely packed case is sandwiched somewhere near the middle of all the other data points reported in Figure 3a. To explain the wide scatter of the data points and to explain the difference in the heat transfer from its linear variation in Ra as given by Equation 8, many theories were put forth. A thorough discussion on the causes and possible reasons for this behaviour can be found in Nield and Bejan (1992).

Transient experiments: oscillating bottom wall temperature

The second major objective of this research was to determine the effect that a time-dependent bottom wall boundary condition has on the heat transfer through the horizontal porous layer. To this end 49 transient experiments were conducted. Of these experiments, the cavity was filled to the top with beads (completely packed case) in 19 of the runs (Table 3) but had a small visible gap at the top in the remaining 30 runs (Table 4).

The bottom wall temperature was modulated using the electrical circuit discussed earlier. The bottom wall temperature varied cyclically with the runs having a period of 6, 12, 23, 46, 92, or 183 min (set by the timer) and for each period selected, the external resistance was changed between the runs to vary the amplitudes of the temperature swing. For example, inspecting Table 3 we see that runs 3, 7, and 11 had the same period, $P = 46$ min, but the amplitudes of the temperature swings were 8.5, 15.6, and 32.3 percent of the enclosure mean temperature difference (fourth column, Table 3), respectively.

The measured bottom wall temperature variation as a function of time for six typical runs are plotted in Figures 5a–f.

Table 3 Transient experiments with oscillating bottom temperature: completely packed case

Run	Period (min)	$\overline{\Delta T}$ (°C)	AMP/$\overline{\Delta T}$	Ra	$\overline{Nu}_{cycle}$	Nu_{ss}	$\overline{Nu}_{cycle}/Nu_{ss}$
1	11.44	23.66	0.036	455.4	8.80	7.11	1.238
2	22.79	23.34	0.060	433.9	8.83	6.79	1.301
3	45.56	23.87	0.085	462.0	9.06	7.21	1.257
4	91.33	23.88	0.091	451.1	8.82	7.04	1.253
5	182.63	24.81	0.103	472.7	9.05	7.36	1.229
6	11.41	24.44	0.066	455.6	9.13	7.11	1.281
7	45.48	24.52	0.156	453.9	9.19	7.08	1.297
8	91.00	24.11	0.173	450.2	9.22	7.03	1.311
9	22.72	23.99	0.173	471.4	9.21	7.35	1.253
10	22.81	22.49	0.242	631.5	9.81	9.71	1.010
11	45.84	22.29	0.323	622.9	9.97	9.58	1.040
12	91.50	21.37	0.419	584.3	10.32	9.02	1.144
13	22.81	29.64	0.073	967.2	14.98	14.60	1.026
14	91.37	26.04	0.196	794.8	13.09	12.10	1.082
15	183.17	25.68	0.207	782.0	13.45	11.91	1.129
16	22.83	24.33	0.054	660.6	9.09	10.14	0.891
17	22.83	23.75	0.055	653.4	8.95	10.04	0.893
18	45.78	23.55	0.073	647.9	9.27	9.96	0.937
19	45.72	24.11	0.079	647.8	9.30	9.95	0.934

In each of these figures, both instantaneous and mean (cycled-averaged) temperatures are shown for the bottom wall. The instantaneous temperatures are shown by the square symbols, and the solid lines represent the mean temperatures. Two different cases are shown in these figures. Figures 5a–c correspond to the case of constant period but different amplitude bottom plate temperature oscillation, and Figures 5d–f represent experiments with nearly the same amplitude but having different periods.

Inspection of Figures 5a–c shows that, for a fixed period, the bottom wall temperature time history looks qualitatively the same over the range of amplitude tested and takes on a sawtooth appearance in shape. Increasing the amplitude of the temperature oscillation "stretches" the scale of the y-axis and the sawtooth profile becomes more distinctive. More interesting are Figures 5d–f, which show the bottom wall temperature time dependence for experiments having approximately the same amplitude but different periods. It can be

Table 4 Transient experiments with oscillating bottom temperature: clear top-layer case

Run	Period (min)	$\overline{\Delta T}$ (°C)	AMP/$\overline{\Delta T}$	Ra	$\overline{Nu}_{cycle}$	Nu_{ss}	$\overline{Nu}_{cycle}/Nu_{ss}$
1	11.58	18.70	0.043	466.3	11.29	11.45	0.986
2	22.83	19.72	0.072	510.3	11.12	12.33	0.902
3	45.75	19.68	0.088	507.2	11.10	12.27	0.905
4	91.72	19.91	0.101	508.6	11.03	12.29	0.898
5	11.46	19.90	0.080	526.6	11.23	12.64	0.888
6	22.79	19.76	0.138	516.5	11.23	12.45	0.902
7	90.67	22.26	0.284	446.5	10.36	11.06	0.937
8	182.60	22.00	0.325	434.8	10.61	10.82	0.981
9	22.83	20.45	0.267	464.0	10.85	11.41	0.952
10	45.81	20.26	0.378	449.4	10.98	11.11	0.988
11	91.88	20.91	0.445	435.5	10.74	10.83	0.991
12	5.69	20.76	0.080	483.4	10.91	11.79	0.925
13	11.41	28.01	0.054	740.7	15.97	16.70	0.956
14	22.71	28.18	0.075	749.2	15.93	16.85	0.945
15	45.71	28.08	0.082	747.8	16.01	16.83	0.952
16	91.17	27.88	0.099	737.9	15.95	16.65	0.958
17	182.67	28.07	0.102	743.9	15.93	16.76	0.951
18	11.45	28.10	0.113	750.5	15.95	16.88	0.945
19	34.08	25.63	0.193	642.2	14.41	14.86	0.969
20	45.72	27.80	0.180	727.7	15.85	16.46	0.963
21	91.33	27.71	0.216	727.4	15.97	16.45	0.971
22	183.0	27.35	0.237	712.8	16.27	16.18	1.006
23	5.72	28.25	0.083	760.8	16.01	17.06	0.938
24	11.52	26.86	0.157	733.1	16.61	16.56	1.003
25	22.87	27.37	0.221	734.2	16.25	16.56	0.981
26	91.25	27.32	0.299	712.8	16.33	16.18	1.009
27	5.73	28.13	0.120	758.8	16.14	17.03	0.948
28	11.44	27.95	0.214	747.0	16.25	16.81	0.966
29	22.78	27.33	0.325	721.8	16.66	16.35	1.020
30	45.63	26.83	0.406	692.1	17.03	15.80	1.078

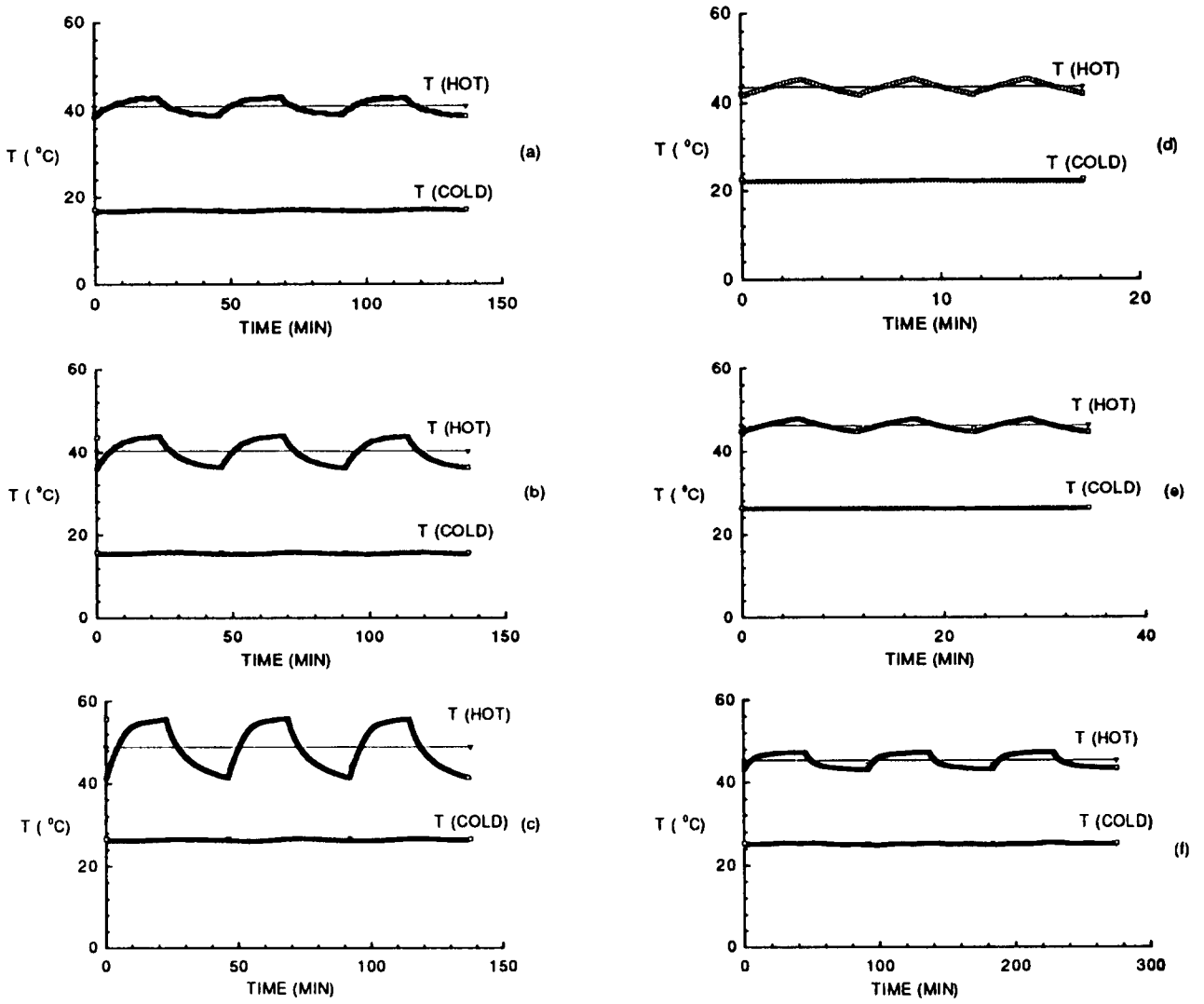

Figure 5 Measured bottom-plate temperature variation with time for typical experiments. Runs with constant period and changing amplitude (see Table 3): (a) run 3; (b) run 7; and (c) run 11. Nearly the same amplitude but different periods (see Table 4): (d) run 12; (e) run 5; and (f) run 4

noticed that for short periods (less than 11 min, Figures 5d–e) the instantaneous temperature of the bottom plate is always changing. In the case of longer periods (more than 91 min, Figure 5f) the temperature of the bottom plate initially increases within the cycle but then tends to become constant. Thus, the bottom plate temperature profile is triangular for the case of short periods but shows distinctive plateaus for long periods. The cold plate temperature is constant in the case of a shorter period (Figures 5d–e) but shows slight variation with time for the longer period (Figure 5f).

The Rayleigh numbers of the transient experiments are reported in the fifth column of Tables 3 and 4 and were based on the temperature difference $\overline{\Delta T}$ between the mean hot wall and the mean cold wall values as

$$\overline{\Delta T} = \overline{T_h} - \overline{T_c} \tag{9}$$

with the thermophysical properties used in the Ra definition evaluated at the arithmetic average of the mean top and mean bottom plate temperatures. The cycle-averaged Nusselt number $\overline{Nu}_{cycle}$ is reported in the sixth column in Table 3 and

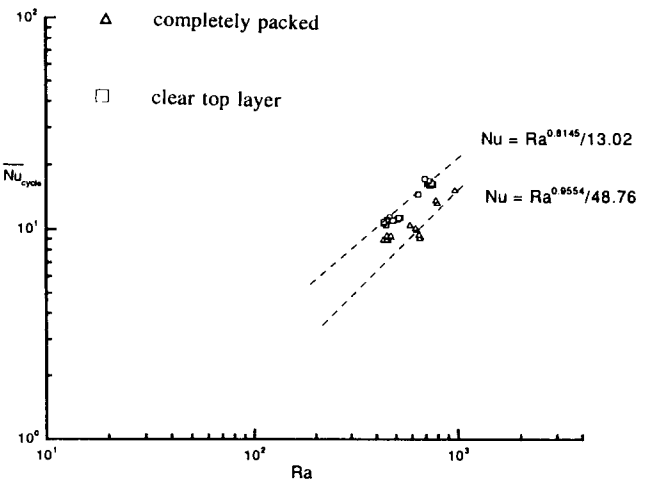

Figure 6 $\overline{Nu}_{cycle}$ *vs* Ra for the transient oscillating bottom wall temperature experiments

is the main sought after result of the experiments. For the sake of comparison, the steady-state Nusselt number Nu_{ss}, based on the same exact mean temperature difference, is located just to the right and was determined from the steady-state correlations derived earlier. Nu_{ss} listed in Table 3 was calculated using Equation 7 and Nu_{ss} in Table 4 via Equation 6.

The ratio $\overline{Nu}_{cycle}/Nu_{ss}$ is tabulated in the last column of Tables 3 and 4 and is greater than unity if the heat transfer is larger through the enclosure with unsteady wall temperature than with constant temperature walls, and is less than unity if the temperature modulation causes a reduction in the average heat transfer through the layer.

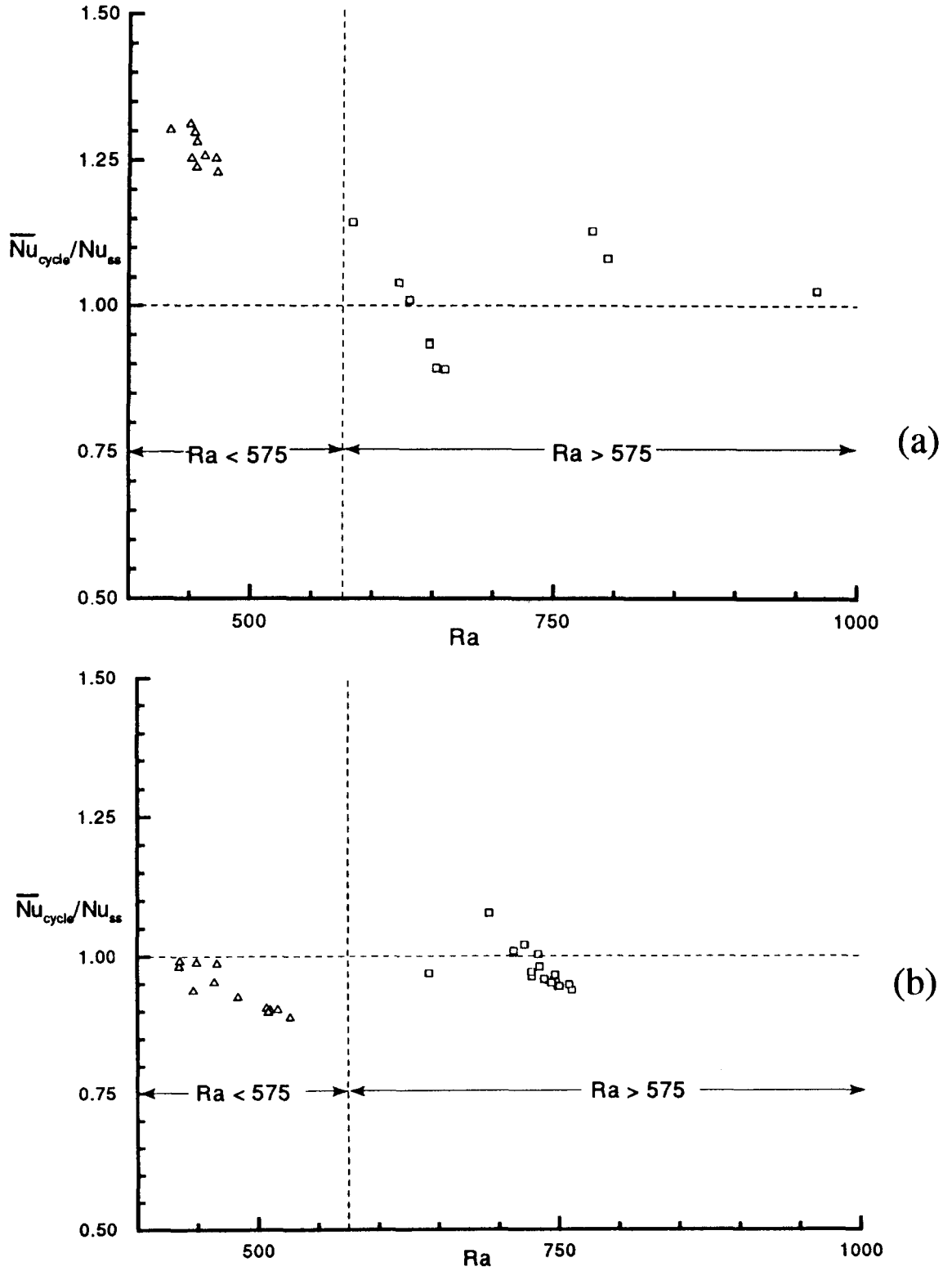

Figure 7 $\overline{Nu}_{cycle}/Nu_{ss}$ *vs* amplitude ratio for the transient oscillating bottom wall temperature experiments: (a) completely packed; and (b) clear top layer

Nusselt number *versus* Rayleigh number for the transient data is plotted in Figure 6 for both the completely packed case (triangular symbol) and the clear top-layer (square symbol) experiments. The dashed lines shown in Figure 6 are the steady-state correlations reported earlier in Figure 4. Comparing transient data to steady-state predictions shows that there exists a measurable deviation in the heat transfer from the steady-state value caused by the wall temperature oscillations. For the clear top-layer case (square symbols), the heat transfer is consistently lower at smaller Ra values but is scattered about the steady-state value at the higher Ra ranged tested. Conversely, the completely packed top results (triangular points) show that the heat transfer is considerably greater at the low end, compared with its steady-state value, and becomes closer to it as Ra increases. For Ra between $600 < Ra < 650$ (the group of 5 triangular points located near

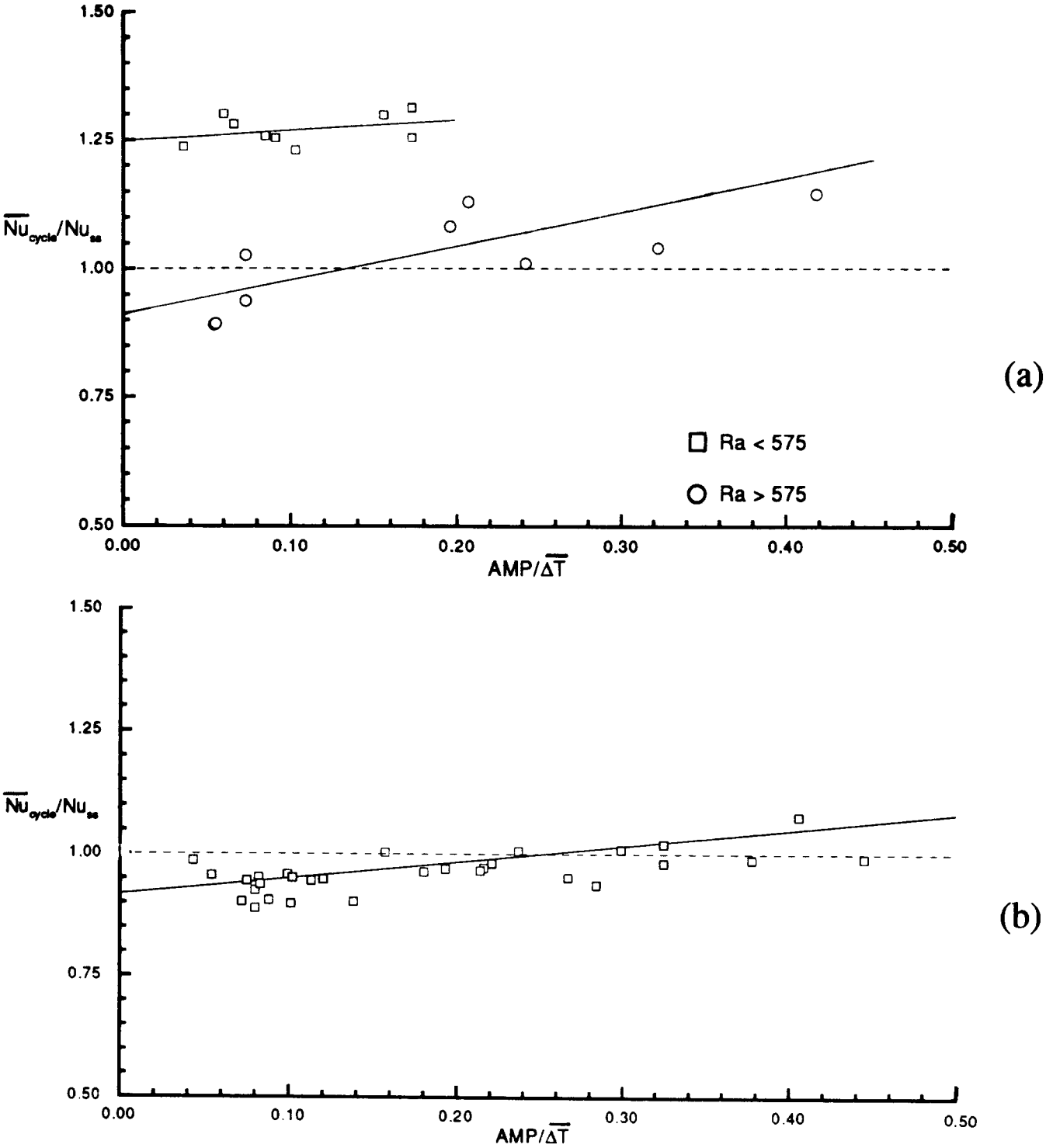

Figure 8 $\overline{Nu}_{cycle}/Nu_{ss}$ *vs* amplitude ratio for the transient oscillating bottom wall temperature experiments: (a) completely packed; and (b) clear top layer

the middle) the heat transfer can either be lower or higher than the steady-state value.

The deviation in the heat transfer from its steady-state value, as a function of Ra number, is shown more clearly in Figure 7. The transient data points located above the horizontal line, $\overline{Nu}_{cycle}/Nu_{ss} = 1$, show an increase in the heat transfer, whereas those points falling below the line exhibit a reduction in heat transfer. Comparison of the upper with the lower figure shows that the wall temperature oscillation affects the heat transfer differently, depending on the type of top boundary condition. For Ra < 575, enhancement occurs in the enclosure without a gap (Figure 7a), but wall temperature oscillation lowers the heat transfer through the enclosure if a gap exists (Figure 7b). Also, we see from Figure 7 that there is a much stronger Ra dependence in the top figure (completely packed case) than in the bottom figure (clear top-layer data). The heat transfer ratio

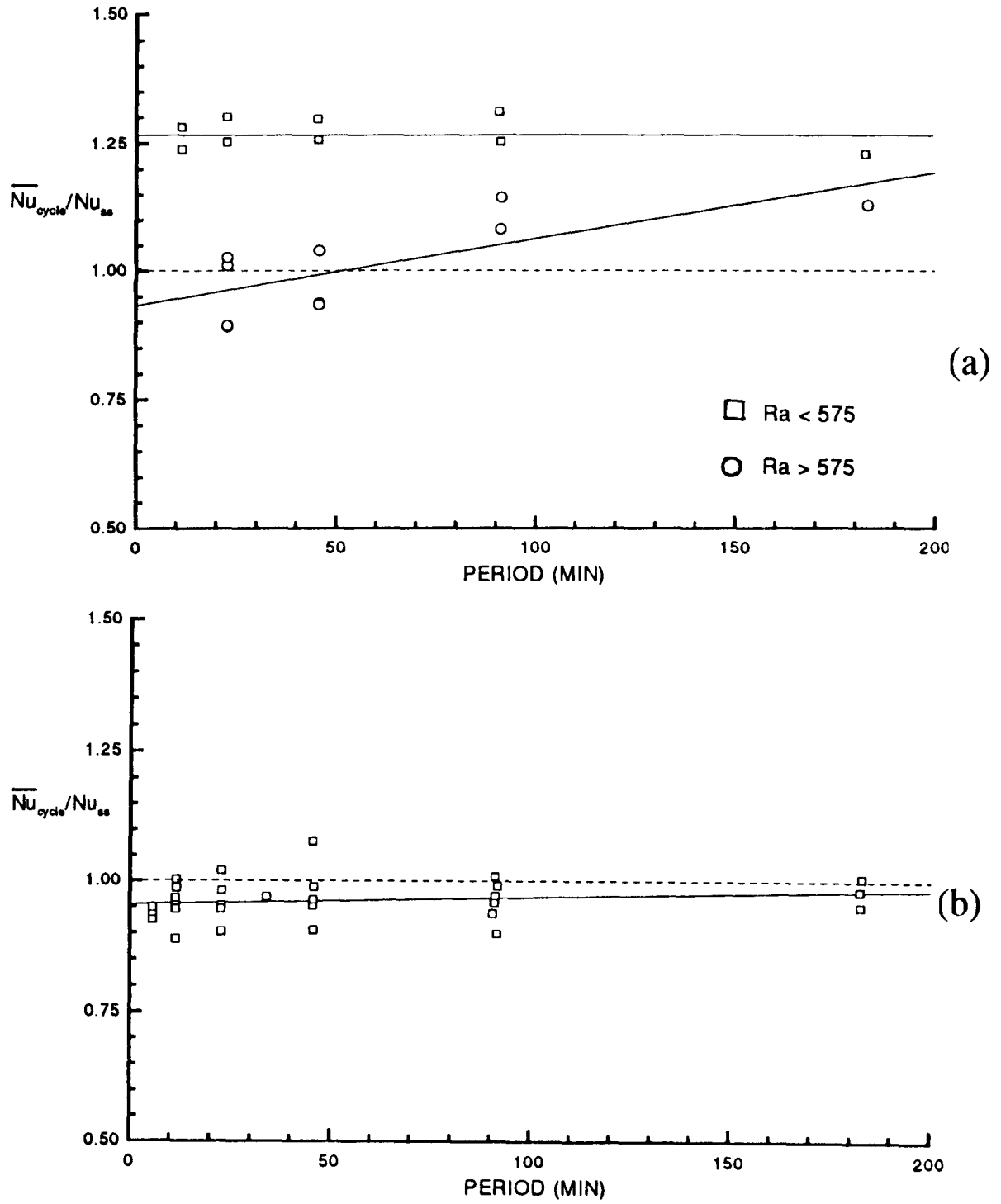

Figure 9 $\overline{Nu}_{cycle}/Nu_{ss}$ *vs* period for the transient oscillating bottom wall temperature experiments: (a) completely packed; and (b) clear top layer

appears to be almost Ra insensitive in the enclosure that has a thin gap and behaves basically the same over all Ra values tested.

To understand the oscillating bottom wall temperature influence on the heat transfer better, the ratio $\overline{Nu}_{cycle}/Nu_{ss}$ is plotted as a function of the dimensionless amplitude ratio $Amp/\overline{\Delta T}$ in Figure 8 and is plotted *versus* period P in Figure 9. The Ra dependence is isolated to some extent in these figures by considering select points only in exploring the trends. For example, for the completely packed data, runs with $Ra < 575$ and runs with $Ra > 575$ are treated as two separate groups. This distinction was not made for the clear top-layer data (the lower plots in Figures 8 and 9) because Ra appears not to be an important factor when a gap is found over the beads (Figure 7b).

Basically, Figures 8 and 9 show that the heat transfer ratio does indeed depend on the amplitude ratio and on the period of the wall temperature modulation. Figures 8 and 9 show that the greater the value of these parameters, the higher the heat-transfer ratio. This behavior is true for both upper surface conditions, but note, overall, that there is still a net decrease in the heat-transfer rate for the clear top-layer case (lower figures) compared with its steady state, whereas generally we find a net increase in the rate of heat transfer for the completely packed enclosure (upper figures).

Finally, comparing Figure 8 with Figure 9 reveals two additional facts. First, the heat-transfer ratio correlates somewhat better with the amplitude ratio than it does with the period (note how the data points fall closer to the best-fit line in Figure 8 compared with Figure 9). Second, the heat-transfer ratio $\overline{Nu}_{cycle}/Nu_{ss}$ depends more strongly on the amplitude ratio than it does on the period (compare the slopes of the solid lines between the two figures). However, Figures 8 and 9 are not independent from one another. To explain, the data plotted in Figure 8, showing the amplitude dependence, include runs with different periods, whereas the data shown in Figure 9, illustrating the period dependence on the heat-transfer ratio, have data with variable amplitude ratio. Unfortunately, to develop an accurate heat-transfer correlation of the form,

$$\overline{Nu}_{cycle}/Nu_{ss} = f(Ra, Amp/\Delta T, period) \quad (10)$$

where each parameter dependence is explicitly derived, requires many more experiments to be performed.

Conclusion

Twenty-five steady-state and 49 transient natural convection experiments were conducted on a horizontal porous layer heated from below. In all of the experiments, the porous matrix consisted of 3-mm glass spheres saturated with distilled water. The temperatures of the top and bottom walls were maintained constant in the steady-state experiments, but the bottom wall temperature oscillated in a cyclic fashion in the transient experiments.

Analysis of the steady-state experiments showed that the presence of a small gap at the top surface of the enclosure increases the steady-state heat transfer through the enclosure. In addition, the data also show that the gap may lessen the Rayleigh number dependence on the steady-state heat transfer through the layer.

Transient experiments conducted in a porous layer for both completely packed and clear top-layer upper surfaces revealed that the wall temperature oscillation cause the cycled-average heat transfer to deviate from its steady-state value. Overall, it was found that the wall temperature modulation predominantly enhances the heat transfer for an enclosure without a gap but tends to reduce the heat transfer in the cavity that contained one. For both upper boundary conditions tested, the heat-transfer ratio was shown to be an increasing function of the period and the amplitude of the wall temperature oscillation.

References

Bejan, A. 1984. *Convection Heat Transfer*. Wiley, New York, 412–413

Buretta, R. J. and Berman, A. S. 1976. Convective heat transfer in a liquid saturated porous layer. *J. Appl. Mech.*, **43**, 249–253

Caltagirone, J. P. 1975. Thermal convective instabilities in a horizontal porous layer. *J. Fluid Mech.*, **72**, 269–287

Caltagirone, J. P. and Fabrie, P. 1989. Natural convection in a porous medium at high Rayleigh numbers. Part I— Darcy's model. *Eur. J. Mech.*, **8**, 207–227

Cheng, P. 1978. Heat transfer in geothermal systems. *Adv. Heat Trans.*, **14**, 1–105

Chhuon, B. and Caltagirone, J. P. 1979. Stability of horizontal porous layer with timewise periodic boundary conditions. *J. Heat Trans.*, **101**, 244–248

Combarnous, M. A. and Bories, S. A. 1975. Hydrodynamic convection in saturated porous media. *Adv. Hydrosci.*, **10**, 231–307

Elder, J. W. 1967. Steady free convection in a porous medium heated from below. *J. Fluid Mech.*, **27**, 29–48

Elder, J. W. 1968. The unstable thermal interface. *J. Fluid Mech.*, **32**, 66–69

Ergun, S. 1952. Fluid flow through packed columns. *Chem. Eng. Progr.*, **48**, 89–94

Holst, P. H. and Aziz, K. 1972. Transient three-dimensional natural convection in confined porous media. *Int. J. Heat Mass Transfer*, **15**, 73–90

Kaviany, M. 1984. Thermal convective instabilities in a porous medium. *J. Heat Transfer*, **106**, 137–142

Kladias, N. and Prasad, V. 1989a. Convective instabilities in horizontal layers heated from below: effect of grain size and its properties. *ASME HTD*, **107**, 369–379

Kladias, N. and Prasad, V. 1989b Natural convection in horizontal porous layer: Effects of Darcy and Prandtl numbers. *J. Heat Transfer*, **111**, 926–935

Kladias, N. and Prasad, V. 1990. Flow transitions in buoyancy-induced non-Darcy convection in a porous medium heated from below. *J. Heat Transfer*, **112**, 675–684

Lage, J. L. 1992. Comparison between the Forchheimer and the convective inertia terms for Bernard convection within a fluid saturated porous medium. *ASME HTD*, **193**, 49–55

Lein, H. and Tankin, R. 1992. Natural convection in porous media-nonfreezing. *Int. J. Heat Mass Transfer*, **35**, 175–186

Lister, C. R. B. 1990. An explanation for the multivalued heat transport found experimentally for convection in a porous medium. *J. Fluid Mech.*, **214**, 287–320

Mantle-Miller, W. J., Kazmierczak, M. and Hiawy, B. 1992. Natural convection in a horizontal enclosure with periodically changing bottom wall temperature. *ASME HTD*, **198**, 49–56

Nield, D. A. 1968. Onset of thermohaline convection in a porous medium. *Water Resources Res.*, **2**, 553–560

Nield, D. A. 1992. Estimation of the stagnant thermal conductivity of saturated porous media. *Int. J. Heat Mass Transfer*, **34**, 1575–1576

Nield, D. A. and Bejan, A. 1992. *Convection in Porous Media*. Springer-Verlag, New York

Poulikakos, D. and Renken, K. 1987. Forced convection in a channel filled with a porous medium, including the effects of flow inertia, variable porosity, and Brinkman friction. *J. Heat Transfer*, **109**, 880–888

Ribando, R. J. and Torrance, K. E. 1976. Natural convection in a porous medium: effects of confinement, variable permeability, and thermal boundary conditions. *J. Heat Transfer*, **98**, 42–48

Schubert, G. and Straus, J. 1979. Three-dimensional and unsteady convection in fluid-saturated porous media at high Rayleigh numbers. *J. Fluid Mech.*, **94**, 25–38